

3D Electrodes from aluminium foams prepared by replication process

Horacio Salavagione · Richard Prieto ·
Emilia Morallón · Javier Narciso

Received: 16 April 2009 / Accepted: 16 August 2009 / Published online: 29 August 2009
© Springer Science+Business Media B.V. 2009

Abstract Aluminium foams with pores displaying both regular size and distribution have been prepared by replication methods. Their volumetric density and electrical conductivity were 0.65 g cm^{-3} and 2.44 MS m^{-1} , respectively. This method represents a simple way to produce 3D metal macroporous electrodes. In addition, the aluminium foam has been employed as support to produce 3D platinum electrodes (Pt/Al foam) by electrodeposition. The conditions for platinum electrodeposition have been established, and the electrodes were characterized by scanning electron microscopy and cyclic voltammetry. The electrocatalytic behaviour of the Pt/Al foam electrodes to methanol oxidation has been tested in $1 \text{ M CH}_3\text{OH} + 0.5 \text{ M H}_2\text{SO}_4$ solutions.

Keywords Aluminium foam · Electrocatalyst · Platinum

1 Introduction

Porous materials containing tailored porosity exhibit special properties that cannot be usually achieved by employing

conventional dense materials. Therefore, porous materials nowadays find many applications in several technological processes [1].

Commercial metal foams are mainly constituted by closed cells with diameters from one to several millimetres that are irregular in size and shape [2]. The main application of these materials is in the absorption of energy especially from impacts. However, for certain applications like sound attenuation and filters, open cells are essential and a higher control of the foam microstructure is required [3].

Open-cell metallic foams can be easily produced by the pressure infiltration technique where a solid material is used as a pore shaping template. The molten metal is then poured followed by removal of the template by dissolution. This method, which is known as “replication process” was developed in the late 1960s for the production of metal foams, mostly aluminium [3–5]. However, this process was also developed for the production of mesophase pitch carbon foams [6]. This procedure has several advantages over other production of metal foams [2, 7]; both the pore shape and their distribution are mainly controlled by the initial shape of the solid powder template used to produce the infiltrated preform obtaining uniform and fine open-cell foams [8].

Metal foams have the advantages of monolithic materials (reduction of pressure drop, ease of handling, mechanical stability, etc.), and they can be used as structural supports for catalysts. Moreover, metal foams have high surface area, low density and high thermal conductivity. Thus, the use of metal foams offers interesting possibilities as three-dimensional (3D) catalyst support structures for different applications, for example in electrochemical applications. In the case of electrodes for fuel cell applications, both the support and the electrocatalyst must have high efficiency and electrochemical stability [9–12].

H. Salavagione · E. Morallón (✉)
Departamento de Química Física and Instituto Universitario
de Materiales, Universidad de Alicante, Apdo. 99,
03080 Alicante, Spain
e-mail: morallon@ua.es

R. Prieto
Departamento de Física Aplicada and Instituto Universitario
de Materiales, Universidad de Alicante, Apdo. 99,
03080 Alicante, Spain

J. Narciso
Departamento de Química Inorgánica and Instituto Universitario
de Materiales, Universidad de Alicante, Apdo. 99,
03080 Alicante, Spain

Porous materials have been widely studied as catalyst supports. In the specific case of aluminium, Moskovits et al. have extensively studied the preparation of metal and semiconductor particles on anodic aluminium oxide (AAO) films [13–16]. The authors used a general process that involves the preparation of AAO by anodizing aluminium sheets or foils followed by the application of AC electrolysis of the anodized aluminium in an appropriate electrolyte containing metal ions. Through these studies, the authors have shown that they can control the size of the AAO pores creating uniform nanostructures that can function as nano-templates for metal and semiconductor nanoparticles.

Moreover, Rolison et al. have reported the use of electrocatalyst-modified aluminosilicate zeolites to perform redox chemistry in microheterogeneous media [17]. The metal nanoparticles behave as nanoelectrodes. This has in turn improved the catalytic turnovers relative to the zeolite-free electrocatalyst, generated practical amounts of electrosynthesized product at nanoelectrode-modified zeolites and allowed for selective conversion of reagents to products in high yield.

In this sense, this study focuses on the preparation of metal aluminium foams by a new replication process that uses a solid pattern as template for the metal. This method has the capacity to produce metal foams with controlled porosity (volume and pore shape). In addition, the aluminium foams were employed as support to produce 3D platinum electrodes by electrochemical deposition. This method represents a simple way to produce 3D macroporous electrodes. The pore size is controlled by the conditions of the replication process.

It is well known that platinum is used as a catalyst in numerous organic reactions. Therefore, minimizing the amount of catalyst by supporting it on more cost-effective metal surfaces will improve the efficiency (i.e. the active surface increases) and reduce the costs of the process. In that sense, we propose the use of aluminium foams as 3D supports to electrochemically grow thin platinum films and therefore, to produce high area platinum electrodes.

2 Experimental

The template used was NaCl powder supplied by Fluka Chemie GmbH (purity: 99.5%). NaCl particles were packed into quartz tubes of 16-mm inner diameter and 10-cm length, by vibration. Each packing step consists of the following: approximately 0.25 g of NaCl were added and subjected to vibration for 2 s. The process was repeated until the compact column reached a height of approximately 5 cm. The upper part of the compacted solid was plugged with alumina paper to avoid unpacking of the

preform and partially skim off the oxide layer formed during the melting stage. In order to determine the particle volume fraction (V_p), the quartz tube was weighed before and after the powder was packed inside it, and its outer diameter measured at five points along its length. Using these data, and the length of the packed powder, a V_p of $0.61 \pm 0.01 \text{ cm}^3$ was obtained. The density of the NaCl particles used in this determination was 2.17 g cm^{-3} .

The infiltration equipment used was described in detail elsewhere [18] which consists of: (a) melting and infiltrating under vacuum and inert atmospheres, respectively, and (b) directional solidification of the infiltrated sample. Once the crucible was placed into the chamber, a vacuum of 50 Pa was attained by means of a rotary pump, followed by the injection of nitrogen up to a pressure of 0.1 MPa. Cycles of vacuum and pressure were repeated several times to purge the system from any residual air. Melting at 700 °C was performed under a 100-Pa nitrogen atmosphere. Subsequently, metal infiltration was induced by increasing the system pressure with nitrogen gas up to 1 MPa and maintaining it for at least 2 min. After solidification, the template was removed with distilled water. Figure 1 shows the experimental procedure used to obtain 3D Pt/Al foam electrodes.

The morphology of the electrodes was analysed using a Hitachi S-3000 N scanning electron microscope (SEM) that was coupled to a Rontec X-ray detector for energy dispersive X-ray microanalysis (EDX).

Before platinum electrodeposition, the aluminium support (foam or sheet) was cleaned by dipping in a concentrated HCl solution (Merck p.a.) (50% w/v) for 30 s. The aluminium support was then rinsed with ultrapure water under sonication.

The electrodeposition of platinum was carried out in a typical three electrode electrochemical cell using 0.5 M $\text{Na}_2\text{HPO}_4 + 10^{-3} \text{ M H}_2\text{PtCl}_6$ electrolyte [19] (final pH = 6.8) under potentiostatic conditions. The aluminium support (foam or sheet) was used as the working electrode, while a Ag/AgCl/Cl^- (sat.) electrode and a graphite electrode of high area were used as reference and counter electrode, respectively. The potential was kept at $-0.5 \text{ V vs Ag/AgCl/Cl}^-$ (sat.) for different electrodeposition times. After platinum electrodeposition, the Pt/Al electrodes (Pt/Al foam and Pt/Al sheet electrodes) were rinsed with ultrapure water.

In all the electrochemical measurements, the reference electrode used was a Ag/AgCl/Cl^- (sat.) electrode.

The Pt/Al foam electrodes were tested in 0.5 M H_2SO_4 and 0.5 M $\text{H}_2\text{SO}_4 + 1 \text{ M CH}_3\text{OH}$ electrolytes by cyclic voltammetry. For comparison purposes, bare platinum electrode (Pt) and platinized aluminium sheet electrode (Pt/Al-sheet) were also studied at the same conditions as the 3D Pt/Al foam electrodes.

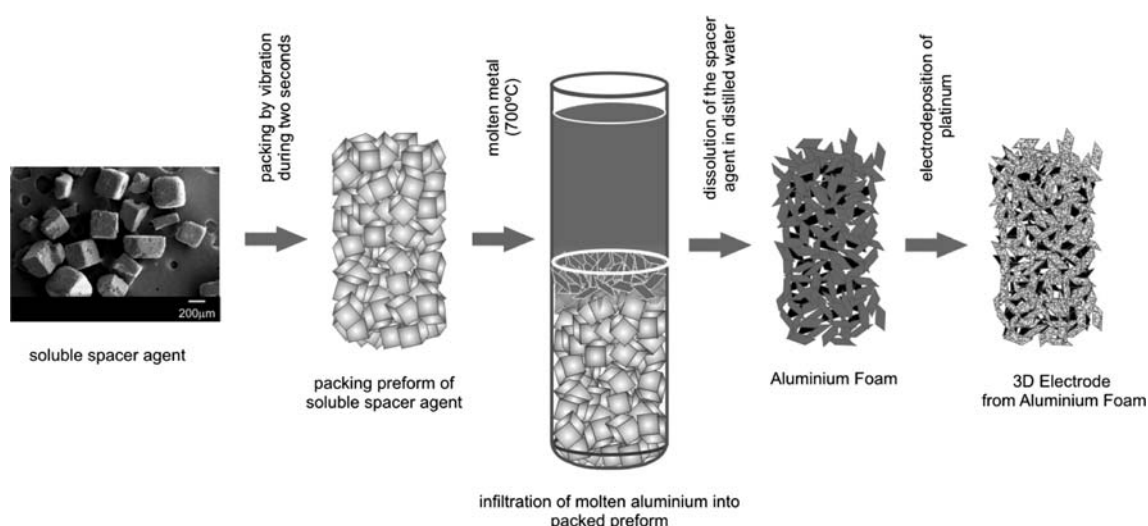


Fig. 1 Scheme of the experimental procedure to obtain 3D platinum supported on aluminium foam

3 Results and discussion

Figure 2 shows a SEM image of the aluminium foam support obtained by the method described in the experimental section before platinum electrodeposition. The cubic porosity observed corresponds to the space occupied by the original NaCl template. The observed maximum pore size was between 0.4 mm and 0.6 mm. The volumetric density (measured by the Archimedes method) and electrical conductivity (measured using Eddy current) were 0.65 g cm^{-3} and 2.44 MS m^{-1} , respectively.

Aluminium foam electrodes were subjected to several platinum electrodeposition times maintaining the deposition potential to find the best conditions for obtaining stable platinum particles (the times used were 15, 30, 45, 60 and 120 min). For electrodeposition time of 45 min and beyond, a similar platinum distribution was obtained; however, for lower deposition times, no stable platinum films were observed.

Figure 3a and b show the images obtained using back-scattered radiation of the Pt/Al-foam electrode obtained after 45 min of electrodeposition at -0.5 V . A homogeneous distribution of platinum particles on the metal aluminium foam can be observed. Figure 3b shows a detailed view in which a cauliflower-like structure of the platinum particles is observed. In order to prove that the shiny parts in the SEM images correspond to platinum, EDS analysis was performed (Fig. 3c), and Pt was detected together with Al. In addition, the presence of oxygen was also detected suggesting the formation of Al_2O_3 which decreases the number of active sites for Pt electrodeposition (the measured O/Al ratio is 1 in wt/wt, the theoretical ratio being 0.89). However, the presence of Al_2O_3 in the surface could be helpful regarding the stability of the electrode because it

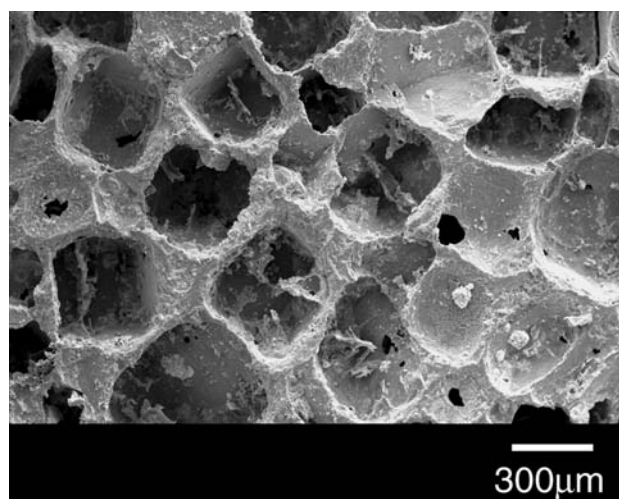
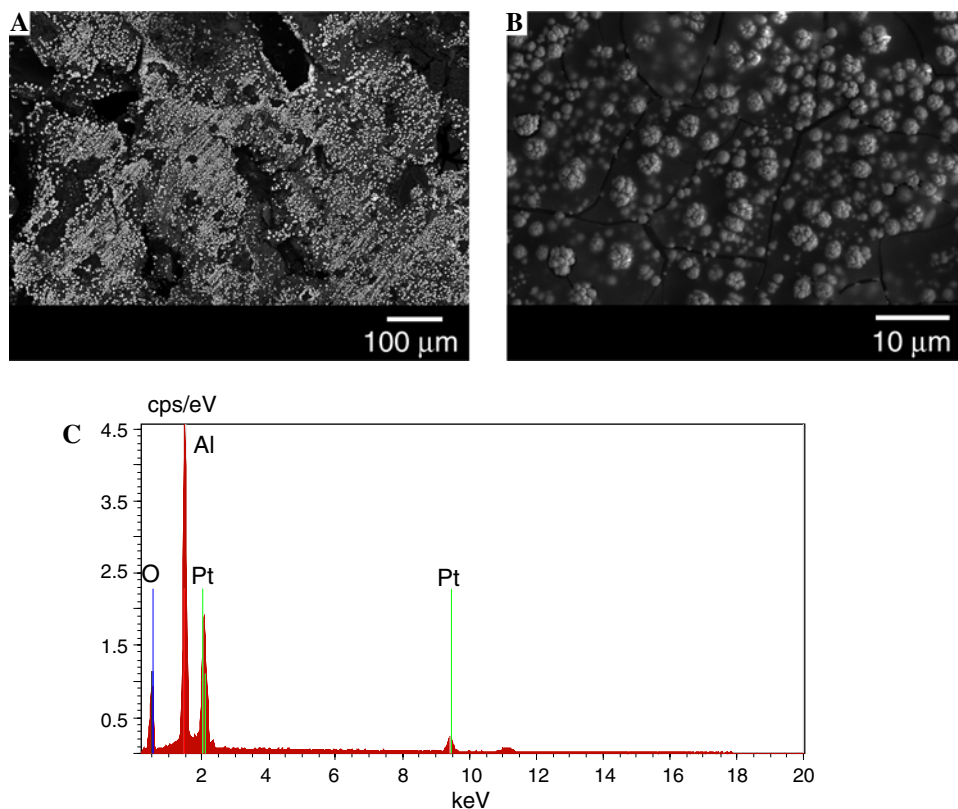


Fig. 2 SEM images of aluminium foam produced by replication process

passivates the aluminium surface not covered with Pt, thus avoiding its dissolution. It has been checked that the platinum particles are inside the aluminium foam obtaining a cross-sectional image of the Pt/Al foam (figure not shown).

The electrochemical behaviour of the Pt/Al-foam electrode was analysed in a sulphuric acid solution. Figure 4 shows the cyclic voltammogram for the Pt/Al-foam electrode after 45 min of electrodeposition at -0.5 V (dashed line). The cyclic voltammograms were acquired at a scan rate of 50 mV s^{-1} until stable response was obtained. The voltammogram exhibits the characteristic features expected for a platinum electrode. The region between -0.2 V and 0.2 V corresponds to the so-called hydrogen adsorption-desorption zone. During the anodic sweep, oxygen adsorption is first observed at about 0.6 V , which

Fig. 3 SEM images of Pt/Al-foam at lower (a) and higher (b) magnifications and c EDX results of the analysis of image b



corresponds to the formation of platinum surface oxide. During the cathodic sweep, the reduction peak of the platinum surface oxides, located at about 0.47 V, is also observed [20, 21]. For comparison purposes, Figure 4 also shows the voltammograms for both a bare Pt electrode (dashed line) and a Pt/Al-sheet electrode (solid line) obtained under the same conditions as the Pt/Al foam

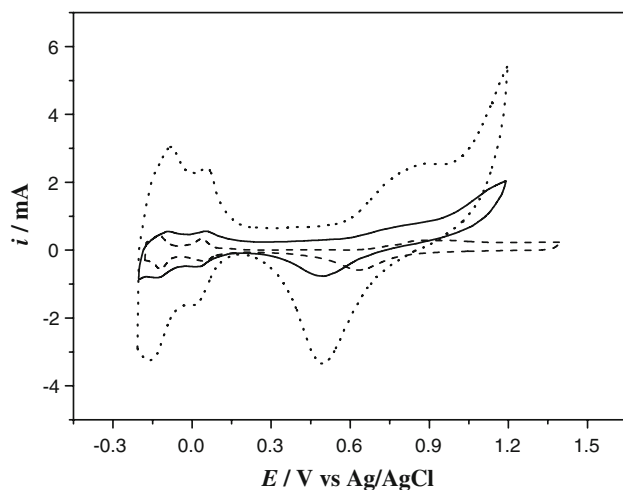


Fig. 4 Steady cyclic voltammograms of bare Pt electrode (dashed line), Pt/Al-sheet electrode (solid line) and Pt/Al-foam electrode (dotted line) in 0.5 M H_2SO_4 solution. $\nu = 50 \text{ mV s}^{-1}$. The y-axis for the Pt electrode (dashed line) has been multiplied by ten

electrode. It can be seen that the electrochemical response is very similar, but the electrical charge measured between -0.20 and 0.25 V is lower than that in the case of a Pt/Al-foam electrode (note that the dashed line corresponds to a ten-time amplified original signal). Therefore, it was confirmed that the platinum particles were successfully created into the 3D structured aluminium foams.

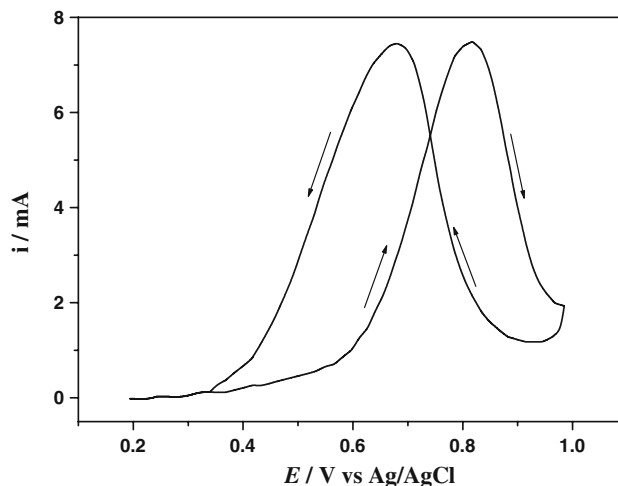


Fig. 5 Cyclic voltammograms of Pt/Al-foam electrode in 0.5 M $\text{H}_2\text{SO}_4 + 1 \text{ M CH}_3\text{OH}$ solution. $\nu = 50 \text{ mV s}^{-1}$

Table 1 Values of current at $t = 0, 0.2$ s and 100 s during chronoamperometric experiments, and percentages of deactivation at 100 s referred to the current at 0 and 0.2 s for the Pt/Al-sheet and Pt/Al-foam electrodes

Electrode	$i_{t=0}$ (mA)	$i_{t=0.2}$ (mA)	$i_{t=100}$ (mA)	Deactivation $_{t=0}$ (%)	Deactivation $_{t=0.2}$ (%)
Pt/Al- foam	6.4	4.6	4.3	32	7
Pt/Al- sheet	0.024	0.172	0.010	58	40

1 M CH₃OH + 0.5 M H₂SO₄ solution

The active surface area (ASA) of the Pt/Al-foam electrode defined as $\text{m}^2 \text{g}^{-1}$ Pt, was calculated from the voltammogram in Fig. 4 using the following equation [22]:

$$\text{ASA} = \frac{Q}{m_{\text{Pt}} q_{\text{H}}^0}$$

where Q is the electric charge (C) obtained from the integrated area of the adsorption–desorption region in the voltammogram between -0.20 V and 0.25 V (subtracting the double-layer contribution), m_{Pt} is the loading of Pt (g) determined by the chronoamperogram considering the total reduction to Pt of the hexachloroplatinic acid (PtCl_6^{2-}), and q_{H}^0 is the electric charge for a monolayer of one electron adsorption–desorption process on Pt ($210 \mu\text{C cm}^{-2}$). The value obtained for Pt/Al-foam electrode is $29 \text{ m}^2 \text{g}^{-1}$; this value is lower than those reported for platinum nanoparticles supported on carbon materials (being around $72 \text{ m}^2 \text{g}^{-1}$ for Vulcan, and $90 \text{ m}^2 \text{g}^{-1}$ for carbon nanofibers [21, 23]). However, this value is reasonable taking into account that the pores in the aluminium foam support have dimensions of micrometers.

In order to check the behaviour of these electrodes in a reaction test, the electrochemical oxidation of methanol on the Pt/Al-foam electrode in acidic medium has been studied. The voltammogram obtained (Fig. 5) is very similar to that observed for platinum electrodes at the same conditions [24, 25]. However, the current peak and the ratio between the current for the forward scan (I_f) and the backward scan (I_b), which are related to carbon dioxide and carbon monoxide produced by methanol oxidation, respectively [26], diminished with the number of cycles. The I_f/I_b ratio is almost 30% lower after 40 min of cycling [27]. Thus, the decrease of the I_f/I_b value suggests that the catalyst is becoming less efficient.

Chronoamperometric experiments have also been performed at 0.8 V for Pt/Al-foam and Pt/Al-sheet electrodes obtained in the same electrodeposited conditions. These current–time experiments have been used to follow the kinetics in platinum single crystal electrodes [28]. In our case, the potentiostatic current decreases rapidly with time for the two electrodes following diffusion-controlled reaction. Table 1 shows the instantaneous current ($i_{t=0}$), the current at 0.2 s ($i_{t=0.2}$) and the percentages of deactivation after 100 s referred

to $i_{t=0}$ and $i_{t=0.2}$. The higher activity of the Pt/Al-foam electrode, and its lower deactivation can be clearly observed, in agreement with the cyclic voltammetric results.

Thus, the usability of this kind of aluminium foam electrodes as electrocatalysts support has been demonstrated in this report.

4 Conclusions

In summary, a new method to produce aluminium foams has been developed. This method represents a simple way to produce 3D metal macroporous foams that can be used as electrocatalysts support. The aluminium foams have been used as 3D support for electrochemically deposited platinum. The best results were obtained after 45 min of deposit at -0.50 V. The Pt/Al-foam electrode has much higher active surface area than a Pt/Al-sheet electrode obtained under the same conditions or a bare platinum electrode. Thus, using the Pt/Al-foam electrode, a higher efficiency for methanol oxidation in acid medium has been obtained in comparison with Pt/Al-sheet obtained under the same conditions or bare Pt electrodes.

Acknowledgements The authors thank the Ministerio de Ciencia e Innovación, Feder and Generalitat Valenciana (Projects MAT2007-60621 and ACOMP/2009/174) for financial support.

References

1. Studart AR, Gonzenbach UT, Tervoort E, Gauckler LJ (2006) J Am Ceram Soc 89:1771
2. Banhart J (2001) Prog Mater Sci 46:559
3. Degischer HP, Kriszt B (2002) Handbook of cellular metals production, processing applications. Wiley-VCH, Vienna
4. Polonsky L, Lipson S, Markus H (1961) Mod Cast 39:57
5. Despois JF, Mortensen A (2005) Acta Mater 53:1381
6. Parodi MP, Prieto R, Narciso J, Louis E (2006) Carbon Conference, Aberdeen
7. Gibson LJ (2000) Annu Rev Mater Sci 30:191
8. Gaillard C, Despois JF, Mortensen A (2004) Mat Sci Eng A-Struct 374:250
9. Sasaki K, Wang JX, Balasubramanian M, McBreen J, Uribe F, Adzic RR (2004) Electrochim Acta 49:3873
10. Yang W, Yang S, Sun W, Sun G, Xin Q (2006) Electrochim Acta 52:9

11. Skowronski JM, Wazny A (2005) *J Solid State Electrochem* 9:890
12. Sirijaruphan A, Goodwin JG Jr, Rice RW, Wei D, Butcher KR, Roberts GW, Spivey JJ (2005) *Appl Catal A-Gen* 281:1
13. Goad DGW, Moskovits M (1978) *J Appl Phys* 49:2929
14. Pontifex GH, Zhang P, Wang Z, Haslett TL, AlMawlawi D, Moskovits M (1991) *J Phys Chem* 95:9989
15. Routkevitch D, Bigioni T, Moskovits M, Xu JM (1996) *J Phys Chem* 100:14037
16. Preston CK, Moskovits M (1993) *J Phys Chem* 97:8495
17. Rolison DR, Bessel CA (2000) *Acc Chem Res* 33:737
18. Prieto R, Molina JM, Narciso J, Louis E (2008) *Scripta Mater* 59:11
19. Pournaghi-Azar MH, Habibi AB (2005) *J Electroanal Chem* 580:23
20. Angerstein-Kozłowska H, Conway BE, Barnett B, Mozota J (1979) *J Electroanal Chem* 100:417
21. Zaragoza-Martín F, Sopena-Escario D, Morallón E, Salinas-Martínez de Lecea C (2007) *J Power Sources* 171:302
22. Woods RJ (1974) *J Electroanal Chem* 49:217
23. Sevilla M, Sanchis C, Valdés-Solís T, Morallón E, Fuertes AB (2007) *J Phys Chem C* 111:9749
24. Iwasita T, Vielstich W (1986) *J Electroanal Chem* 201:403
25. Beden B, Hahn F, Lamy C, Léger JM, de Tacconi NR, Lezna RO, Arví AJ (1989) *J Electroanal Chem* 261:401
26. Yen CH, Shimizu K, Lin YY, Bailey F, Cheng IF, Wai CM (2007) *Energy Fuel* 21:2268
27. Parson R, VaderNoot T (1988) *J Electroanal Chem* 257:9
28. Herrero E, Franaszczuk K, Wieckowski A (1994) *J Phys Chem* 98:5074